

Panama City 2003 Acoustic Coherence Experiments: Low Frequency Bottom Penetration Fluctuation Measurements in a Multipath Environment

Roger W. Meredith, E. Ted Kennedy, Dexter Malley, Robert A. Fisher,
Robert Brown, and Steve Stanic

Naval Research Laboratory, Code 7184, SSC, MS 39529

Abstract. This paper is part of a series of papers describing acoustic coherence and fluctuations measurements made by the Naval Research Laboratory in the Gulf of Mexico near Panama City Beach, FL during June 2003. This paper presents low frequency (1-10 kHz) buried hydrophone measurements and preliminary results for two source-receiver ranges with grazing angles less than two degrees (relative to the direct-path to the seafloor at the receiver location). Results focus on fluctuations after acoustic penetration into the sediment. These fluctuations are correlated with environmental influences.

INTRODUCTION

As given in the earlier paper [1], the omnidirectional G34 transmitted a 4.5 second pulse using a LFM with a low-frequency bandwidth of 500-5000 Hz and a high-frequency bandwidth of 5-12 kHz. Corresponding beamwidths varied from omnidirectional at 1 kHz to approximately 35 degrees at 10 kHz. The G34 has source levels of about 170 dB at 3.5 kHz and was mounted 2.7 m above the sea bottom in approximately 8.8 m of water. The buried receiver was a 6-element, linearly-spaced hydrophone array with a 50 cm aperture. It has a free-field voltage sensitivity (FFVS) of -180 dB re 1V/ μ Pa at 2 kHz and -168 dB at 10 kHz. It was vertically buried at the foot of the vertical low-frequency array. The signals from each hydrophone were cabled back to an instrument canister mounted on the tower. Signals are multiplexed, sent via fiber optic cable to shore, digitized at 100 kHz, and recorded. Data is presented for two source-to-receiver ranges, nominally 70 and 150 m. These correspond to direct path grazing angles of less than two degrees.

An example of the received signals for a single ping on each buried hydrophone is shown in Figure 1. For each acoustic run, five hundred pings were acquired with

greater than 20 dB signal-to-noise ratio, and these pings form the basis for the bottom-penetration fluctuation processing. Channel 1 is the topmost phone and was positioned in the water column on the ocean-sea bottom interface and Channel 6 is the deepest buried phone at 50 cm.

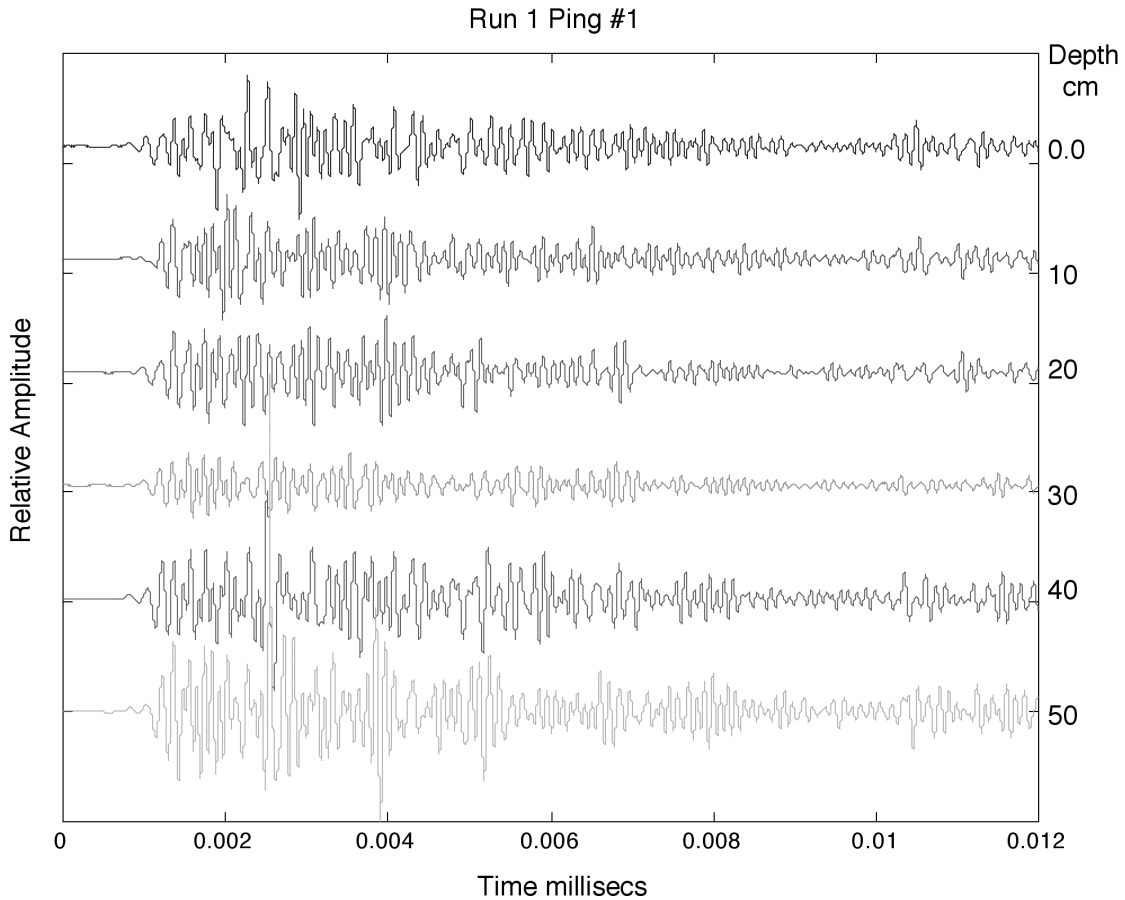


Figure 1. Relative amplitudes for a single ping for each array hydrophone at the short range (~70 m).

Based on the source-receiver geometry for Channel 1 and measured sound speed profiles, an ideal normal mode intensity plot can be generated of the sound field in the water column. Examples are shown in Figure 2 to provide a sense of structure in the sound field. Ray tracing gives more than six arrivals with times less than a pulse length for the short-range geometry.

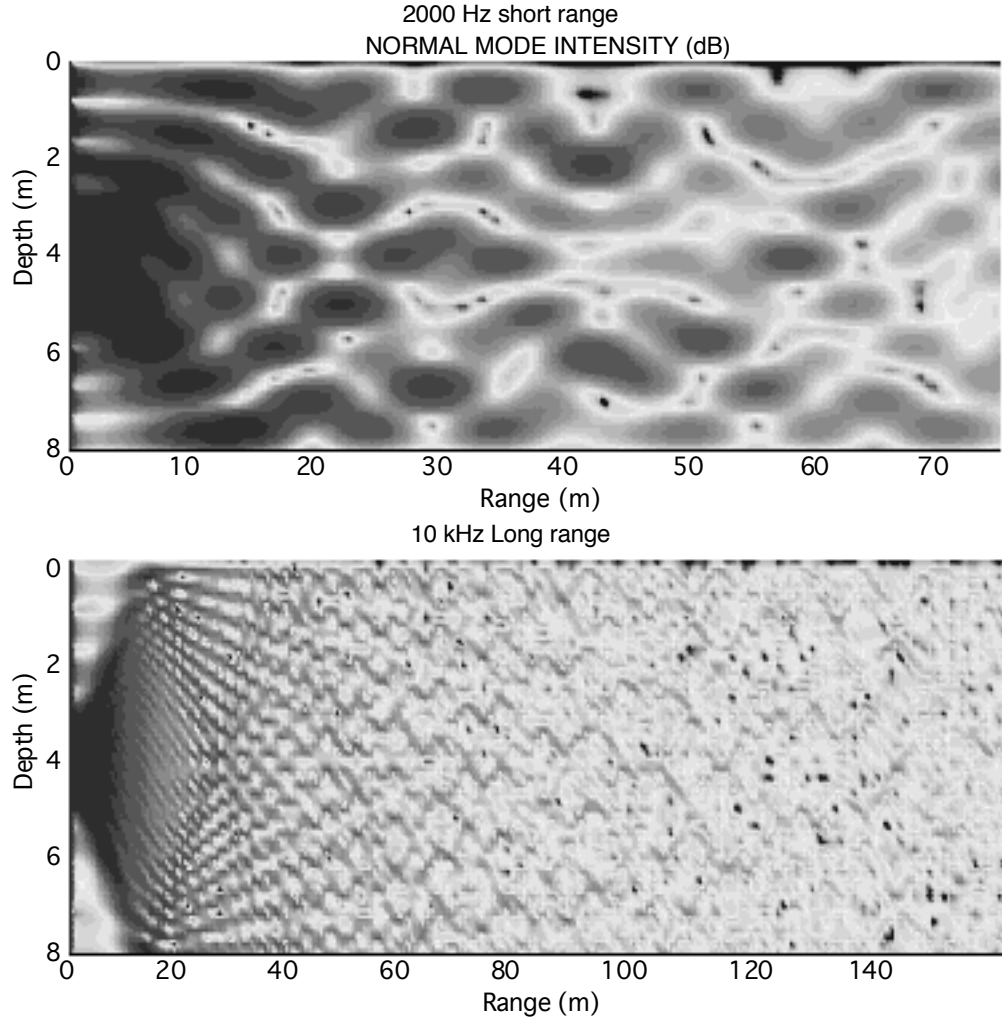


Figure 2. Normal mode intensity plots for the source receiver geometry's using measured sound speed profile averages.

BOTTOM PENETRATION RATIO

This paper focuses on fluctuations in the sediment after acoustic penetration into the bottom sediment. The penetration ratio is a ratio of spectral densities [2, 3] where P is the Fourier transform of the pressure time series from a hydrophone. This ratio represents the pressure produced by unit amplitude of the incident wave and is defined by:

$$P_r(f) \equiv \left| \frac{P_i(f)}{P_{ref}(f)} \right|^2 \quad (1)$$

where f is frequency Hz, and i is an index to the hydrophone array (i.e., burial depth). This frequency-dependent penetration ratio is the ratio of the spectral density from a hydrophone buried in the sediment to the spectral density of a reference hydrophone.

Typically, the reference hydrophone is located in the water column at or slightly above the sea bottom. A negative dB value of the penetration ratio indicates an attenuation of energy (absorption and scattering) relative to the energy at the reference phone. Scattering and reflections may give rise to positive dB values. To minimize the effects from shadowing and reflections from the tower structure, the reference hydrophone for this work was chosen to be the shallowest buried phone (0.10 cm depth) rather than the phone in the water column. Therefore, this ratio represents the acoustic pressure produced by an incident acoustic wave originating inside the sediment, below the water-seabed interface, and is called the post-penetration ratio in Figure 3. Effects such as seafloor scattering, sea-surface movement, thermal microstructure fluctuations, and grazing angle fluctuations are also reduced since these effects occur in the propagation path prior to arriving at the reference phone location.

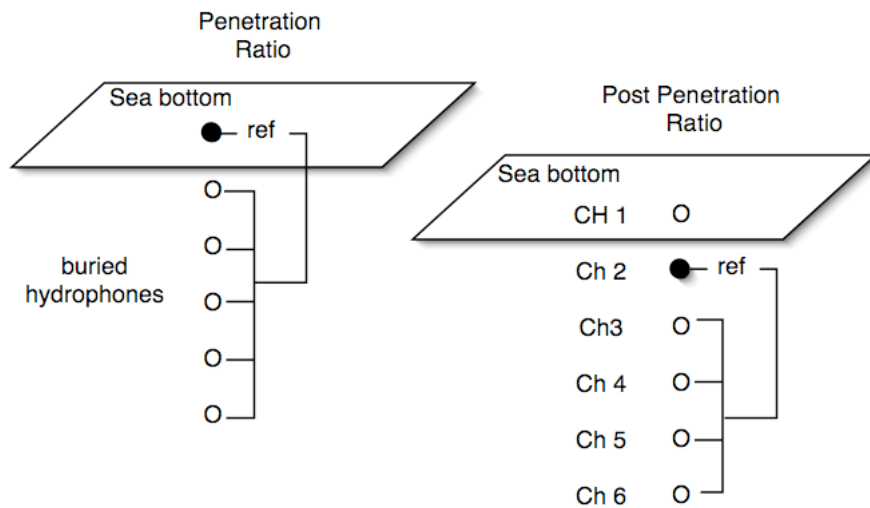


Figure 3. Definition of penetration ratios.

The ping-to-ping amplitude-squared fluctuations of this post-penetration ratio is pursued here to (1) determine the minimum ping-to-ping fluctuations one could expect in the penetration ratio for sandy bottoms, and (2) to determine correlation with environmental influences.

EXAMPLE DATA

A random example of the post-penetration ratio for a single ping is given in Figure 4. The two prominent features of this spectrum are consistent with the penetration ratio and were first explained by Maguer et al. [2, 3]. Their experiments and modeling showed that the linear falloff in the 1-6 kHz band was associated with the evanescent wave propagation. The scalloping in the 6-12 kHz band was associated with Bragg scattering, and sediment-volume scattering. Another noticeable feature of

the post-penetration ratio spectrum is that the relative magnitude (dB) does not decay linearly with depth. This holds for both ranges and is in part attributed to changes in the physical properties and composition of the sediment in both depth and range. Bottom cores from previous experiments indicate that water content and porosity vary actively with depth but are more uniform with range. The quantity of gravel is depth dependent, while sand and clay constituents are more persistent in both depth and range.

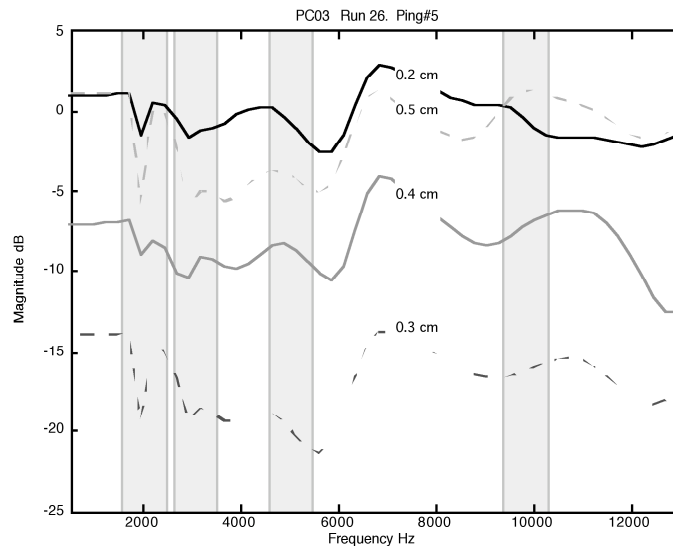


Figure 4. Example of post-penetration ratio for four burial depths for the longer-range geometry.

For this paper, it was necessary to limit the number of frequencies at which ping-to-ping fluctuations would be examined. Four bands were chosen, the beginning, middle, and end of the evanescent wave frequency band and the middle of the frequency band associated with scattering. The mean over a 500 Hz band about each center frequency is computed for each ping to obtain a time series of the post-penetration ratio at each depth. It is with this time series that we begin our analysis of the ping-to-ping relative magnitude fluctuations. An example is shown in Figure 5.

Two metrics chosen to characterize the temporal fluctuations shown in Figure 5, are the standard deviation, (STDEV) and the Gaussian fit error, (GFE). The standard deviation represents the estimate of the error in the mean of the relative magnitude and the Gaussian fit error gives a measure of the deviation from a Gaussian distribution. GFE is the least-square error between the cumulative distribution function of each ping-to-ping time series in Figure 5 and the cumulative distribution function of a Gaussian distribution with the same mean and standard deviation as the ping-to-ping time series. A graphical comparison is given in Figure 6. The symbols are the data probabilities and the line the Gaussian distribution probabilities. Smaller GFE values indicate a more Gaussian distribution.

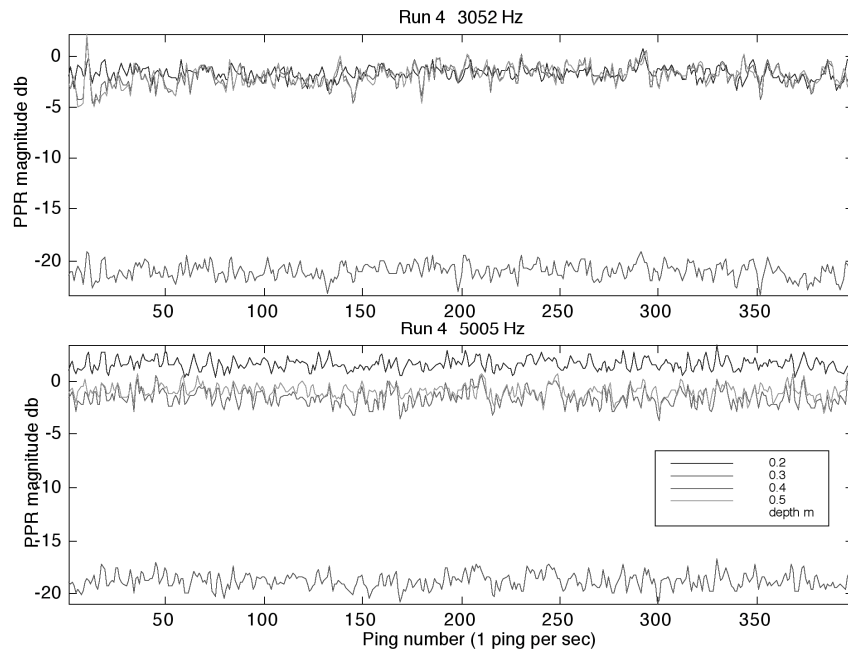


Figure 5. Ping-to-ping time series of post-penetration ratio (PPR) magnitude for two frequency bands for the longer range geometry.

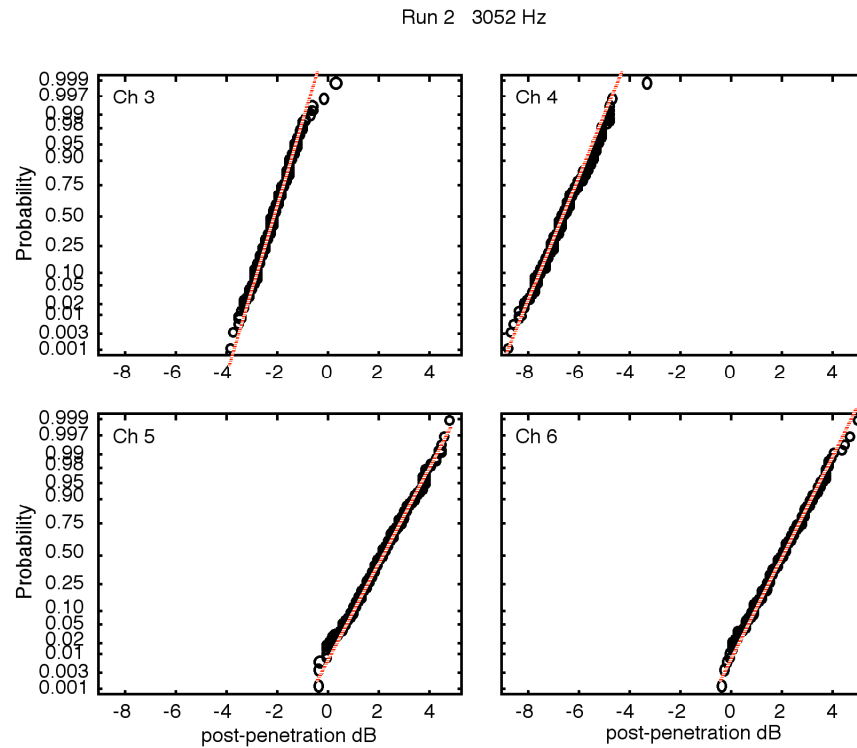


Figure 6. GFE example for single frequency for the shorter range geometry.

RESULTS

The STDEV and GFE of the post-penetration ratio for each buried phone were computed for multiple runs in both the short-range and long-range tower configurations. Each run was approximately 10 minutes in duration. This allowed a sufficient number of pings for comparison with oceanographic conditions to determine the environmental influences on fluctuations. The runs were separated by at least 8 hours and span a total of nine days in June 2003.

Run Number Analysis

Figure 7 shows the STDEV of the post-penetration ratio ping-to-ping fluctuations plotted with run number. Results from all four frequency bands (Figure 7) for each run are included.

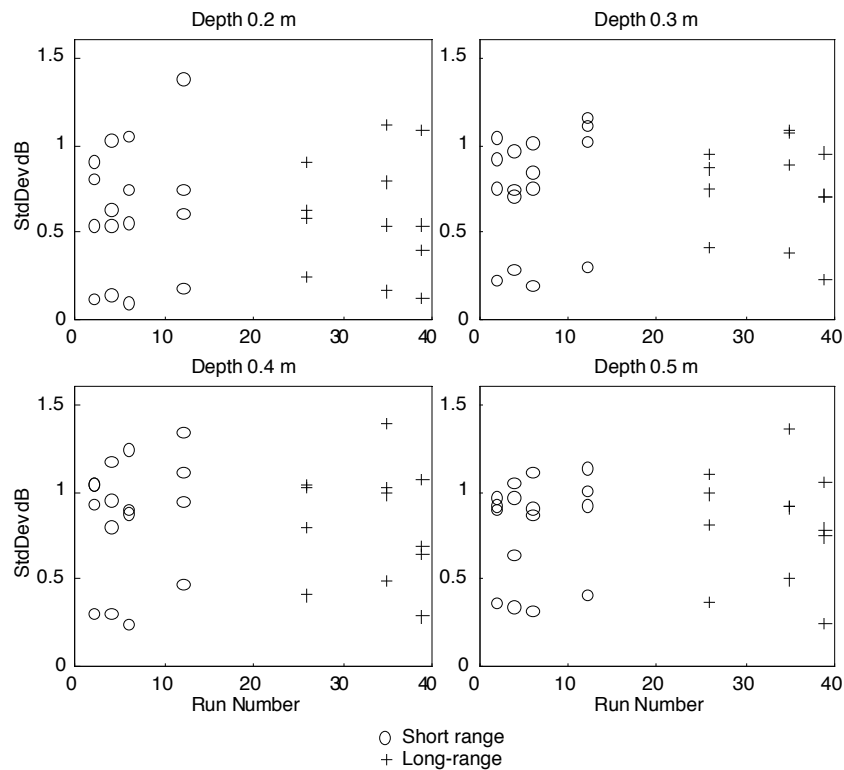


Figure 7. Post-penetration ratio ping-to-ping fluctuations STDEV results .

There is no single run that has the highest or lowest STDEV values for all four depths, but the highest STDEV occurs for runs 12 and 35 for the shorter and longer range respectively. In general, the STDEV is about equal for both ranges. For a threshold of 0.8 dB, the number of occurrences in which the STDEV is greater than the threshold increases with depth to 0.4 m and then levels off. The highest STDEV occurred for Run 35 that correlates with a higher anisotropy index in the TMMS temperatures.

Although not included here, a similar plot was created for GFE vs run number. Overall, the GFE is small. However, run 26 shows a consistently higher GFE for all depths. Otherwise, the GFE is about equal for both ranges. The equality of the results for the two ranges are not unexpected because (1) the direct-path grazing angles are less than two degrees for both ranges, and (2) the number of multipaths are large, and (3) there are multiple interactions with both boundaries for each multipath (Figure 5).

Frequency Band Analysis

Figure 8 shows the STDEV vs frequency band (indicated in Fig. 5) for the post-penetration ratio ping-to-ping fluctuations. Results from all runs at both ranges are included. At the smallest separation (0.2 m depth in Figure 8) from the reference hydrophone, the STDEV increases non linearly with frequency band. For the other three separations, the STDEV is almost constant above 3 kHz. Below 2 kHz, the STDEV is < 0.5 dB.

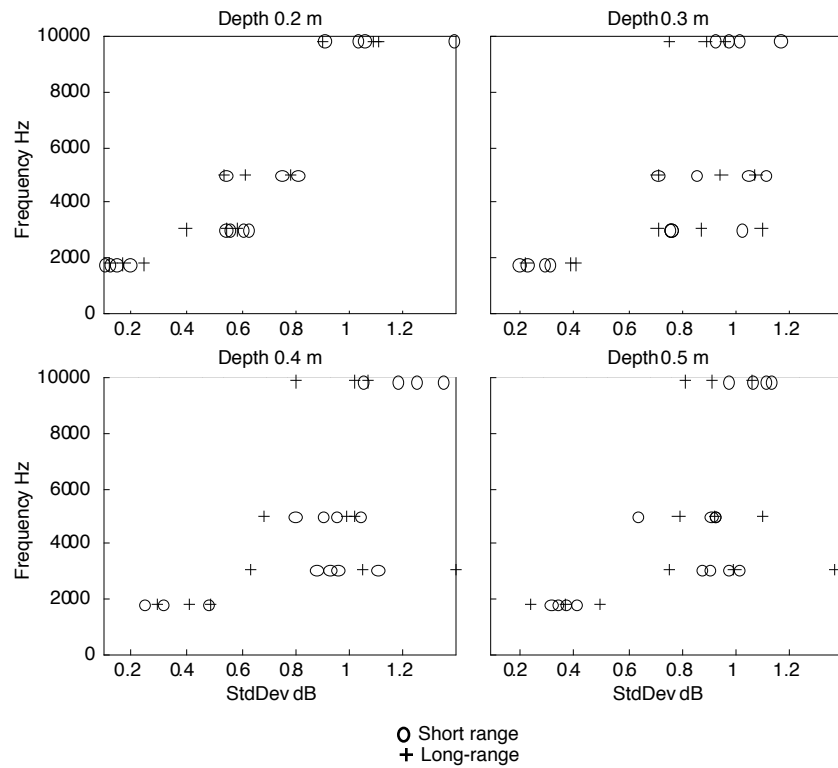


Figure 8. Post-penetration ratio ping-to-ping fluctuations STDEV results with frequency band.

The GFE was found to be small, averaging 0.14, and was insensitive to frequency band for all runs and all depths. This analysis has revealed runs 12, 26, and 35 to warrant further ping-to-ping investigation.

Fluctuation Spectrum Analysis

The Fourier transform of the ping-to-ping time series of post-penetration ratio magnitudes (an example was shown in Figure 5) gives rise to a fluctuation spectrum. Although these spectrums appear to have some structure, they are noisy. A fifth-order low-pass elliptical filter was applied to each spectrum and followed with an ensemble average over all the runs for each range separately. These results are shown in Figure 9 for each of the four frequency bands but is limited to hydrophone CH 3 (0.2 m depth) only, which is the hydrophone closest to the reference phone (see Figure 3).

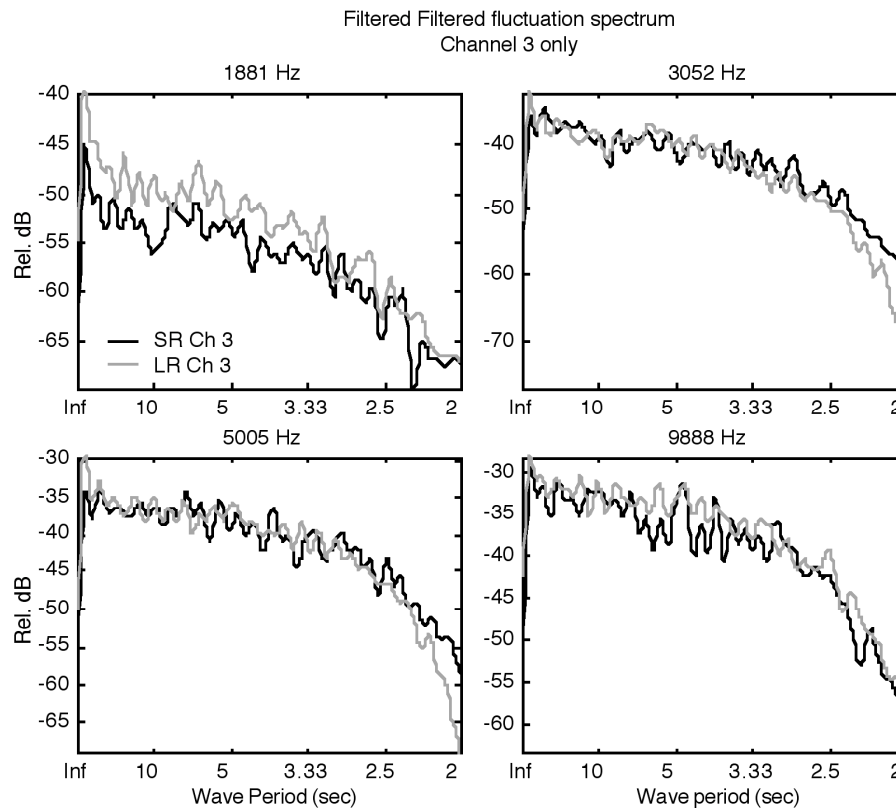


Figure 9. Channel 3 (0.2 m) post-penetration ratio ping-to-ping fluctuation spectrums after low-pass filtering and averaging over runs for each range.

The filtering and ensemble averaging (over runs) reveals some interesting features in the fluctuation spectrum. Only the 1881 Hz band appears to be a linear power-law spectrum. The other frequencies are curvilinear. What stands out in all four frequency bands and at both ranges, are peaks and a slightly raised relative spectral level over the wave periods from 3.5 - 7 seconds, the same range of measured periods for the sea-surface wave spectrum. Even with large number of multipaths, and a large number of surface wave interactions (as indicated in Figure 2), the effects of the moving surface do not average out. Surface effects are more noticeable in the short-range average and perhaps more well defined, although the definition may be filtering effect. Also, the

multiple peaks in the 3.5 - 7 second portion of the post-penetration fluctuation spectrum are consistent with the observation that the measured sea-surface spectrum (computed from a 17 minute time frame) is composed of multiple instances of a sinusoids with different periods not a single periodic wavetrain with multiple periods.

SUMMARY

Among the short range runs, the STDEV of the post-penetration ratio was largest for Run 12, which recorded higher wind speeds, stronger currents, and larger sea-surface wave-heights. The GFE was constant for the short-range runs, and about 10-15% higher for the long-range runs. This correlates with water-column stability. The fluctuations were generally less Gaussian (higher GFE) for stable water conditions (which also coincides with the longer range). The highest STDEV for the long-range runs occurred for Run 35 that recorded the most measured anisotropy index in the TMMS temperature arrays and the smallest sea-surface wave height.

This data has great potential for analyzing environmental effects on ultra-low grazing angle multipath propagation. During the coming year, this data will be modeled using the OASES [4] seismo-acoustic model for comparison with post-penetration ratio measurements. Future data analysis will include cross-correlation as a function of sensor spacing and hydrophone depth for the six-element buried array. This analysis has revealed runs 12, 26, and 35 to warrant further ping-to-ping investigation. The low-level fluctuations in the post-penetration ratio are a result of sea-surface motion.

ACKNOWLEDGMENTS

This research was supported by the Office of Naval Research with technical management by the Naval Research Laboratory under program element 62435N.

REFERENCES

1. Steve Stanic, et.al, "Panama City 2003 broadband shallow-water acoustic coherence experiments," in *Proceedings of the High Frequency Ocean Acoustics Conference*, La Jolla, CA, March 2004.
2. Alain Maguer, Warren L.J. Fox, Henrick Schmidt, Eric Pouliquen, and Edward Bovio, "Mechanisms for subcritical penetration into a sandy bottom: Experimental and modeling results," *J. Acoust. Soc. AM.*, 107 (3), 1215-1225, March 2000.
3. Alain Maguer, Edward Bovio, Warren L.J. Fox, Henrick Schmidt, "In situ estimation of sediment sound speed and critical angle," *J. Acoust. Soc. AM.*, 108 (3), Pt. 1., 987-996, Sept. 2000.
4. Henrik Schmidt, "OASES Version 2.2 User Guide and Reference Manual," Massachusetts Institute of Technology. Cambridge, MA 1999.